Materials Science & Engineering A 636 (2015) 415–420

Contents lists available at ScienceDirect

Materials Science & Engineering A

journal homepage: www.elsevier.com/locate/msea

# $La_2O_3$ effects on TZM alloy recovery, recrystallization and mechanical properties

Kuai-She Wang [a], Jiang-Fei Tan [a], Ping Hu [a,*], Zhi-Tao Yu [a], Fan Yang [a], Bo-Liang Hu [a], Rui Song [a], Huan-Cheng He [a], Alex A. Volinsky [b]

[a] School of Metallurgy Engineering, Xi'an University of Architecture and Technology, Xi'an 710055, China
[b] Department of Mechanical Engineering, University of South Florida, Tampa, FL 33620, USA

ARTICLE INFO

*Article history:*
Received 14 January 2015
Received in revised form
23 March 2015
Accepted 29 March 2015
Available online 8 April 2015

*Keywords:*
Doped lanthanum
TZM alloy
Mechanical properties
Recrystallization
Recovery

ABSTRACT

Titanium, zirconium and molybdenum (TZM) alloy with different amounts of rare earth lanthanum oxide was prepared by powder metallurgy into 0.5 mm thick sheets. The effects of the $La_2O_3$ content on recrystallization temperature and mechanical properties of the TZM alloy were studied. $La_2O_3$ increased the recrystallization and recovery temperature of the TZM alloy and increased its tensile strength and elongation.



## 1. Introduction

Molybdenum is a typical refractory metal, and has excellent high temperature strength, thermal conductivity and corrosion resistance. However, it is brittle at room temperature, has low recrystallization temperature, high plastic to brittle transition temperature and is easily oxidized in air [1–3]. Alloying is a useful way to improve metal performance, and is widely used in molybdenum alloys, including the TZM alloy and rare earth molybdenum alloys. TZM is a Mo-based alloy with 0.5% Ti, 0.06–0.12% Zr and 0.01–0.04% C. Alloying allows overcoming pure molybdenum drawbacks, providing high recrystallization temperature, low plastic-to-brittle transition temperature, excellent high temperature strength, low temperature ductility and improved welding properties. However, TZM alloy recrystallization results in harmful impurity elements present at grain boundaries, which reduce the grain boundary strength. As a result, the molybdenum alloy looses its high temperature performance along with reducing room temperature mechanical properties [4,5], severely limiting the range of TZM alloys applications. Rare earth molybdenum alloys is a branch of widely used molybdenum alloys. Doping with rare earth elements is an effective method to improve molybdenum mechanical properties, including toughness. Dispersion of the rare earth oxides particles in the molybdenum matrix could enhance the strength and ductility of molybdenum, recrystallization temperature and high temperature creep resistance [6,7].

According to the study, the strengthening mechanism [8,9] of TZM alloy are usually three: solid solution strengthening, dispersion strengthening and deformation strengthening. In the molybdenum alloy, the Ti particles play a role of solid solution strengthening, using zirconium carbide or oxide dispersion strengthened, and the deformation strengthening by subsequent pressure processing. Now the more Rare earth oxides are main $La_2O_3$, $Y_2O_3$ and $CeO_2$, and its content is in commonly under 6 vol %. Rare earth oxide has significant influence on room temperature tensile strength, high temperature sag resistance, plasticity, recrystallization temperature [10] and microstructure, etc. In general, the plastic of pure molybdenum after annealing treatment drops rapidly, and shows obvious recrystallization brittleness at room temperature. After joining a certain amount of La2O3, can improve its plasticity, and after high temperature fully recrystallization treatment still has good plasticity.

To further improve the TZM alloy performance, drawing lessons from molybdenum lanthanum rare earth elements alloy reinforcement, the paper studied the effects of $La_2O_3$ on recovery, recrystallization, and mechanical properties of the TZM alloy.

* Corresponding author. Tel.: +86 29 82205096; fax: +86 29 82202923.
*E-mail address:* huping1985@126.com (P. Hu).

http://dx.doi.org/10.1016/j.msea.2015.03.114
0921-5093/

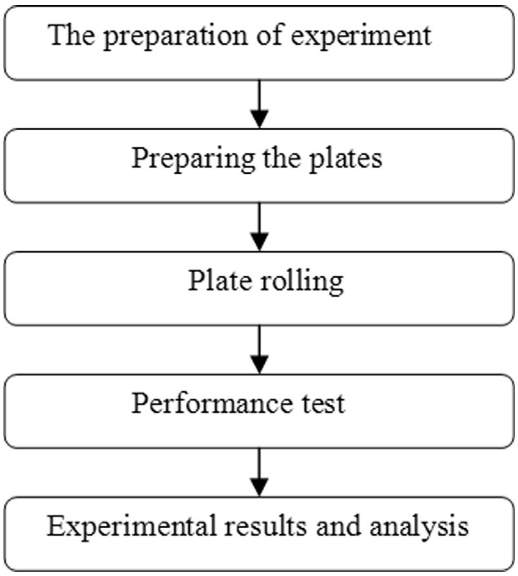


**Fig. 1.** The experimental scheme.

**Table 1**
TMZ alloy composition in wt%.

| Sample | Ti | Zr | C | La | Mo |
|---|---|---|---|---|---|
| 1 | 0.45 | 0.06 | 0.02 | 0 | Rest |
| 2 | 0.45 | 0.06 | 0.02 | 0.10 | Rest |
| 3 | 0.45 | 0.06 | 0.02 | 0.60 | Rest |

## 2. Materials and methods

The main experimental design was as shown in Fig. 1, the experiment process was mainly follows the experimental plan to experiment, and prepared the qualified alloy plate.

### 2.1. Raw materials and processing

Lanthanum-doped TZM alloys were prepared from the following main raw materials: pure Mo powder (Jinduicheng Molybdenum Co., Ltd.), $TiH_2$ powder (Xi'an Baode Powder Metallurgy Co., Ltd.), $ZrH_2$ powder (Xi'an Baode Powder Metallurgy Co., Ltd.), $La_2O_3$ powder (Ganzhou Jiarun New Materials Co., Ltd.), graphite (38 μm maximum granularity). Three samples with different $La_2O_3$ content were made. The slab elements are listed in Table 1, and the preparation process included mixing powder, ball milling, compacting and sintering.

(1) Mixing powder and ball milling
Pure molybdenum powder was mixed with $TiH_2$, $ZrH_2$, $La_2O_3$ and graphite powder, based on the weight percentages listed in Table 1. Then the mixture was ball milled for 24 h, followed by mixing in the three dimensional mixer for 2 h, followed by sieving and vacuum packing.
(2) Compacting
Mould pressing forming technology includes die forming, weighing, pressing, drying, modification and compacting processes. The doped powder was pressed into blanks, pressing, and demoulding after pressure relief got the required shape and size of the products. Steel pressure was 21 Mpa, and the holding time was 5 s, with pressed by one-way.
(3) Sintering
Pressed blanks were pre-sintered in the muffle furnace at 1200 °C for 2 h. Followed by were sintered in the medium frequency induction furnace at 1900 °C for 7 h, with Hydrogen atmosphere.

### 2.2. Rolling and heat treatment

Obtained lanthanum-doped TZM plate was 0.5 mm thick after hot and cold rolling. It was isothermally annealed at 1000–1600 °C for 1 h. The effects of $La_2O_3$ on the recrystallization behavior and mechanical properties of the TZM alloy plate were studied.

### 2.3. Performance testing

The samples were cut out of the rolled plate along the rolling direction using the XQ-2B metallographic specimen mounting press. After polishing and corrosion testing, the samples' microstructure was observed using Nikon SMZ1000 optical microscope. Tensile testing was performed using the WDW-100 10 t tensile machine, and the tensile strength and elongation were obtained. The shape and size of the tensile specimens were based on the ASTM-E8/E8M-08 standards. The tensile samples were cut along the rolling direction. Tensile fracture surface was observed using Hitachi S-3400N scanning electron microscope (SEM) to obtain the fracture and the secondary phase morphology and distribution, analyzing the influence of adding $La_2O_3$.

## 3. Results and discussion

### 3.1. $La_2O_3$ effects on recovery and recrystallization

Microstructure of the Sample 1, without La after annealing at different temperatures is seen in Fig. 2(a), (c), (e), (g) and (i), which show that after 1000 °C annealing Sample 1 has fibrous texture at the recovery stage. At 1200 °C the fibers widen, and tiny recrystallization nucleation appears near the grain boundaries. At 1400 °C the recrystallization process is basically completed and all elongated grains disappear. The microstructure shows equiaxed crystals, which slowly grow with temperature. This was the result that the elongation of sample 1 appeared a larger twist phenomenon after 1400 °C annealing. Fig. 2(b), (d), (f), (h) and (j) show that for the Sample 3, the fibrous texture begins to widen up at 1400 °C. At 1500 °C the wider fibers began to produce tiny crystal nuclei during recrystallization. At 1600 °C, the microstructure is in the form of fully elongated grains, but the lack of equiaxed crystals suggests that the recrystallization is not over yet. Based on Fig. 2, the starting recrystallization temperature of the TZM alloy without $La_2O_3$ (Sample 1) is about 1200 °C. Comparing microstructure of Samples 1 and 3, TZM alloy with 0.6% $La_2O_3$ (Sample 3) has higher recrystallization temperature of about 1500 °C, which is 300 °C higher than without $La_2O_3$ (Sample 1). Adding $La_2O_3$ delays recrystallization significantly.

During the TZM alloy cold rolling, grain slip occurs accompanied by dislocations intertwining, stretching the grain and crushing the fibers, resulting in the TZM alloy work hardening. Adding $La_2O_3$ increases the number of internal defects, making the work hardening phenomenon more obvious. Thus, the non-annealed lanthanum-doped TZM alloy has higher strength and hardness. Cold rolled TZM alloy has high free energy after deformation, which significantly changed its structure, resulting in an unstable state. Thus, the alloy tends towards energy minimization and relaxation. TZM alloy plate deformation at high temperature leads to relaxation, since dislocations have enough energy to move, slide and climb, followed by the sub-grains merging and polygonization [11,12]. High temperature response caused dislocations movement

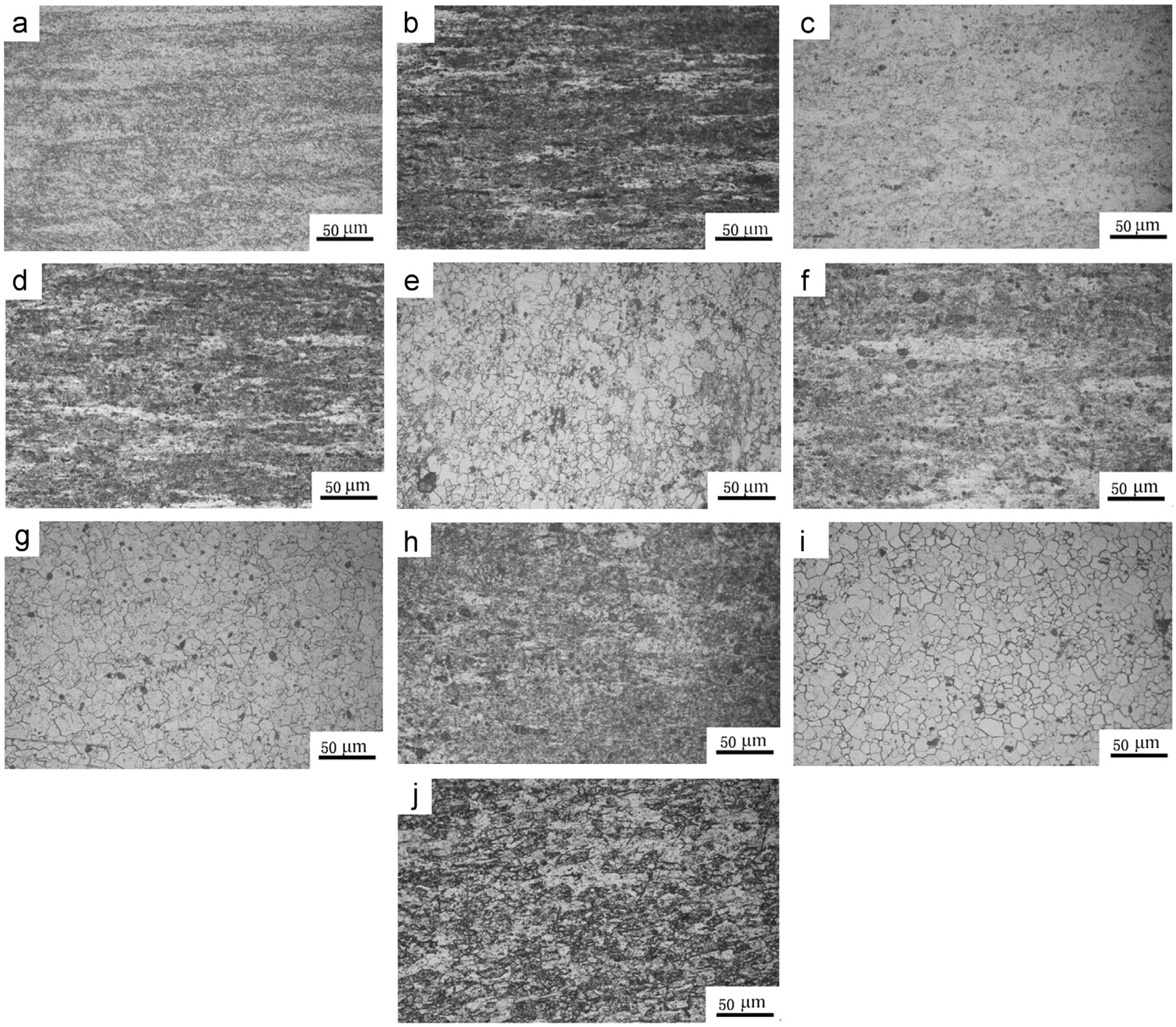


**Fig. 2.** Microstructure of Sample 1 (no $La_2O_3$) annealed at: (a) 1000 °C; (c) 1200 °C; (e) 1400 °C; (g) 1500 °C and (i) 1600 °C and Sample 3 (0.6 wt% $La_2O_3$) annealed at: (b) 1000 °C; (d) 1200 °C; (f) 1400 °C; (h) 1500 °C and (j) 1600 °C.

and decreased dislocation density, although the hardness, strength and plasticity increased. The process of vacancies movement and annihilation does not affect the microstructure, which is significantly changed by dislocation movement. Thus, the movement and rearrangement of dislocations changed the microstructure to mainly polygons and formed the sub-grain [13].

Fig. 2 shows that after 1000 °C annealing, the Sample 1 fibrous texture didn't change, signifying that the low temperature response is mainly due to the movement of point defects. While dislocations or grain boundaries can form at vacancies and interstitials, the hardness and strength didn't change much.

Fibrous texture after 1200 °C annealing explains that the dislocations rearrangement has completed the process of polygons formation, entering the recrystallization process. When the annealing temperature is above 1400 °C, fibrous texture of the Sample 3 is wider. At 1500 °C the recrystallization process began. This suggests that adding $La_2O_3$ particles to the TZM alloy greatly delays the dislocation movement process, accompanied by the pinning effect of the $La_2O_3$ particles, which requires more energy for the dislocation motion. Thus, the recovery process is blocked, requiring higher temperature and more time.

### 3.2. *$La_2O_3$ effect on the recrystallization mechanism*

Molybdenum is a metal with high stacking fault energy, thus recrystallization core will be generated by the sub-grains merging [14]. Deformed metal is the high temperature phase, and the grain boundaries would move, or adjacent grains would merge and grow when the annealing temperature is higher than the recovery temperature. Recrystallization core is based on the small angle crystals produced during recovery. In the recrystallization nucleation stage, small angle grain boundaries near dislocations would form large angle crystals. At the same time dislocations dissolve, producing a large number of vacancies with higher migration rate, thus the recrystallization core would grow rapidly, completing the first phase of the recrystallization. After recrystallization, with the annealing temperature increase, the new growing grains would move on grain boundaries, lowering the distortion energy. This is the second stage of the recrystallization. After adding $La_2O_3$ to the TZM alloy, in the recrystallization nucleation stage, the dislocation slip and aggregation are the leading causes of nucleation. However, $La_2O_3$ particles pin dislocations, and impede their movement, preventing recrystallization nucleation. During the recrystallization grain growth stage, the grains grow, depending on the motion of the grain boundaries. $La_2O_3$ particles along the grain boundaries have a pinning effect, hindering the movement of the grain boundaries, and delaying the recrystallization grain growth process. The pinning mechanism is shown schematically in Fig. 3 [11]. $La_2O_3$ is in the form of spherical particles with the radius of $R_0$. After meeting the grain boundary, $La_2O_3$ particles move, following the process outlined schematically in Fig. 3(a) and (b).

$La_2O_3$ particles partially contact their neighbors and the grain boundaries because of the pinning effect. Thus, $La_2O_3$ particles give rise to an opposite forces with the grain boundary movement, holding the grain boundary, so the grain boundary wants to cross the $La_2O_3$ particles and requires a larger driving force, thus the $La_2O_3$ particles hinder the recrystallization grains growth.

### 3.3. $La_2O_3$ effect on the mechanical properties

Samples 1, 2 and 3, annealed at 1000–1600 °C, were tensile tested. The relationship between the tensile strength and the annealing temperature is shown in Fig. 4, and the relationship between the sample elongation and the annealing temperature is shown in Fig. 5. The tensile strength decreases with the annealing temperature for all samples. The tensile strength of the Sample 1 rapidly decreases from 914 MPa in the as-rolled state to 461 MPa after 1600 °C annealing. The tensile strength of the Sample 2, doped with 0.1% $La_2O_3$ rapidly decreases from 921 MPa in the as-rolled state to 513 MPa after 1600 °C annealing. The tensile strength of the Sample 3 doped with 0.6% $La_2O_3$ rapidly decreases from 963 MPa to 538 MPa. It is also clear that the plate tensile strength significantly increased with the $La_2O_3$ content. On the contrary, the elongation and tensile strength increased with the annealing temperature for the doped samples. The elongation of the un-doped Sample 1 increased from 4.6% in the as-rolled condition to the maximum 31.3% after 1400 °C annealing. However, the elongation dropped rapidly to 10.1% after 1600 °C annealing. After 1400 °C annealing, the elongation of pure TZM alloy appeared a larger twist phenomenon. The elongation of the Sample 2 doped with 0.1% $La_2O_3$ rose from 6.2% in the as-rolled state to 27.7% after 1600 °C annealing. The elongation of the Sample 3 doped with 0.6% $La_2O_3$, similar to the Sample 2, rose from 7.9% to 29.8% after annealing at 1600 °C. However, both elongation of TZM alloy added La2O3 grain did not appear as the larger twist phenomenon as sample 1. Mainly, at 1400 °C, because of the Sample 1 has completed the complete recrystallization, and grain size can coarsen and grow up with the increase of temperature. Which results in the decrease of material of plastic, so the elongation turn and began to reduce after 1400 °C. The recrystallization of the Sample 2 and Sample 3 begins at 1500 °C, and fully recrystallization temperature is above 1600 °C, so the elongation has been on the rise.

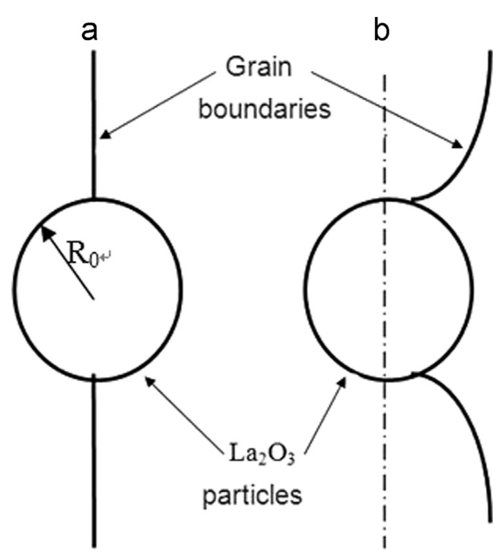


**Fig. 3.** $La_2O_3$ particles effect on the grain boundary migration.

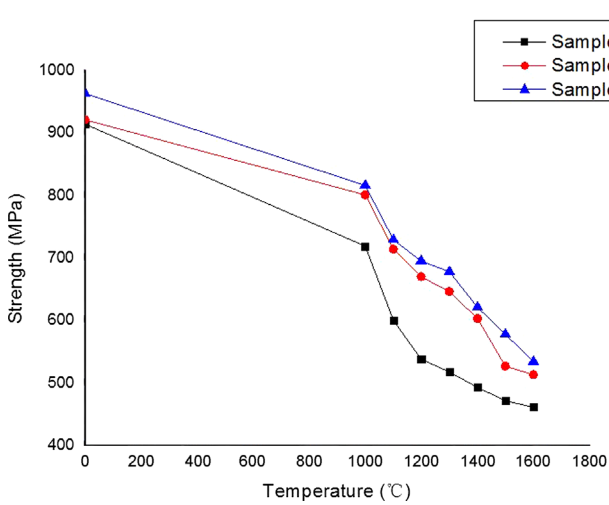


**Fig. 4.** Tensile strength dependence on the annealing temperature.

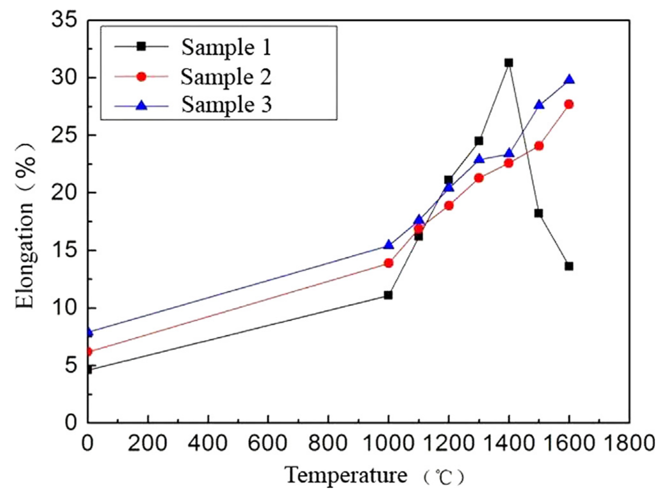


**Fig. 5.** Elongation dependence on the annealing temperature.

### 3.4. The microstructure of TZM alloy doped $La_2O_3$ particles

Tensile fracture surfaces in Fig. 6 show that the reinforcement of $La_2O_3$ particles is mainly due to the strong interactions of the $La_2O_3$ particles with dislocations [15,16]. In the alloy plate a large number of dislocations are firmly pinned by the $La_2O_3$ particles, requiring more stress for the dislocations to overcome the pinning effect. This is the main reason why the tensile strength of the lanthanum-dopes TZM alloy is higher than the pure TZM alloy at room temperature. With the higher $La_2O_3$ content, there is stronger interaction of the particles and dislocation strengthening. This reaction to dislocation pinning effect is also enhanced, and the $La_2O_3$ particles reinforcement is more obvious.

Fig. 7 show that the $La_2O_3$ particles distribute between the transgranular and the grains boundary. The big $La_2O_3$ particles distribute at the grains boundaries, and the small $La_2O_3$ particles in the transgranular. The alloy ductility is increased with the $La_2O_3$ doping due to the dispersion strengthening effect of the $La_2O_3$ secondary phase particles. At the same time, a large number of

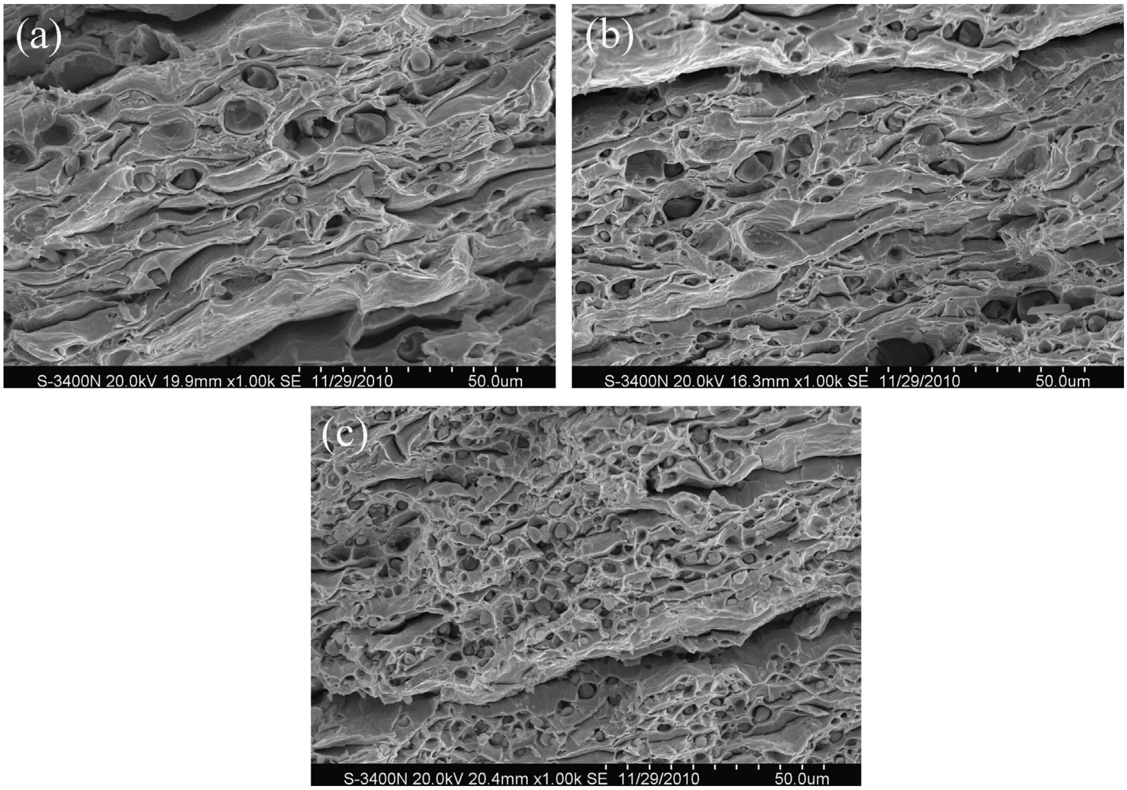


**Fig. 6.** Tensile fracture surfaces of: (a) Sample 1 with no doping; (b) Sample 2 with 0.1% $La_2O_3$ and (c) Sample 3 with 0.6% $La_2O_3$.

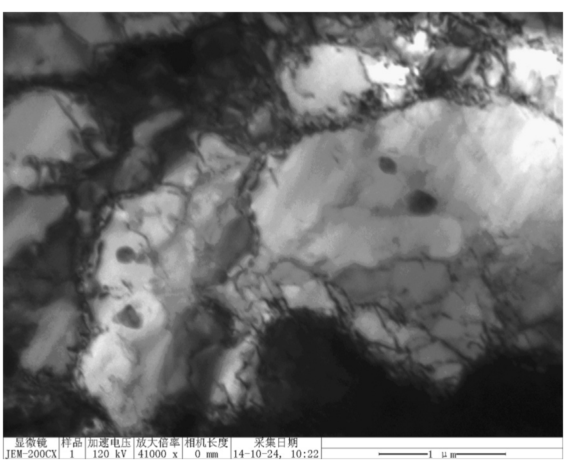


**Fig. 7.** TEM images showing the $La_2O_3$ particles between the transgranular and the grains boundary.

$La_2O_3$ particles in the matrix, or in the grain boundaries hinder the dislocation movement and recrystallization grain growth.

Although a small amount of $La_2O_3$ particles along the grain boundaries could promote intergranular cracks formation, based on the TZM alloy improved strength and elongation, there are no obvious adverse effects. A large number of evenly distributed small dispersed $La_2O_3$ particles can absorb a lot of strain without cracking, forming micropores, causing stress relaxation and at the same time improving the elongation of the alloy.

## 4. Conclusions

(1) Adding $La_2O_3$ to the TZM alloy can significantly delay the recrystallization process, and rise the recrystallization starting temperature. The recrystallization starting temperature of the Sample 1 with no lanthanum doping is 1200 °C. The recrystallization starting temperature of the Sample 3 with 0.6% $La_2O_3$ doping is 1500 °C, which is 300 °C higher than for the Sample 1 (no doping).

(2) $La_2O_3$ particles have a strong pinning effect on the dislocations, and at the same time refine the grain size.

(3) They increase the tensile strength and elongation of the TZM alloy plate. For the same conditions, along with the increase of the $La_2O_3$ content, tensile strength and elongation of the TZM alloy plate are also increased.

## Acknowledgments

The authors acknowledge support from the Major Scientific and Technological Innovation Project of the Shaanxi Province of China (S2011ZK1087), the Science and Technology Innovation Fund Project of the Western Metal Materials Co., Ltd (XBCL-1–06), The Science and Technology as a Whole the Innovation Engineering Planned Project of the Shaanxi Province (2014KTCQ01-35), the Innovation Team Foundation of the Xi'an University of Architecture and Technology.

## References

[1] I.G. Sharma, S.P. Chakraborty, A.K. Suri, J. Alloy Compd. 393 (2005) 122–128.
[2] Y. Hiraoka, T. Hoshika, Int. J. Refract. Met. H 17 (5) (1999) 339–344.
[3] F. Yang, P. Hu, K.S. Wang, J. Alloy Compd. 593 (2014) 196–201.
[4] C. Schimpf, T. Mrotzek, U. Martin, J. Refract. Met. Hard Mater. 28 (2010) 716–721.
[5] P. Hu, K.S. Wang, H.C. He, X.Q. Kang, H. Wang, P.Z. Wang, Appl. Mech. Mater. 320 (2013) 350–353.
[6] M. Endo, The effects of doing molybdenum wire with rare earth elements, in: H. Bildstein, et al., (Eds.), Proceedings of the 13th International Plansee Seminar '89(1), 37, Metallwerk Plansee, Reutte, 1989, p. 52.

[7] A.J. Mueller, R. Bianco, R.W. Buckman, Int. J. Refract. Met. H 18 (2000) 205–211.
[8] Zong-yu Cai, Jian-min Jin, Ye Chen, J. Shanghai Iron Steel Inst. 3 (1993) 56–58.
[9] Zhong Lv, Pei-liang Liu, Ying-hua Xing, et al., J. Iron Steel Res. Inst. 3 (3) (1983) 81–84.
[10] T. Mrotzek, A. Hoffmann, U. Martin, J. Refract. Met. Hard Mater. 24 (2006) 298–305.
[11] W.-X. Song, Metallography [M], Metallurgical Industry Press, Beijing, 1989.
[12] G.I. Zelada-Lambri, O.A. Lambri, P.B. Bozzano, J.A. García, C.A. Celauro, J. Nucl. Mater. 380 (2008) 111–119.
[13] Y.-N. Xu, Principles of Metallography [M], Metallurgical Industry Press, Beijing, 2000.
[14] Y.-Q. Pao, Metallography Basis [M], Metallurgical Industry Press, Beijing, 1986.
[15] J. Zhang, L. Liu, M. Zhou, Y. Hu, T. Zuo, J. Refract. Met. Hard Mater. 17 (1999) 405–409.
[16] C. Chen, S. Wang, Y.L. Jia, M.P. Wang, Z. Li, Z.X. Wang, J. Alloy Compd. 589 (2014) 531–538.